

Fig. 2 Jet centerline velocity decay.

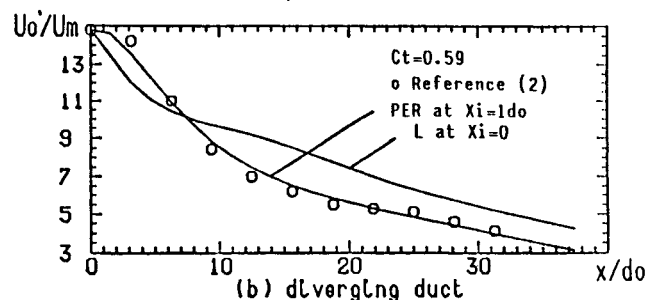
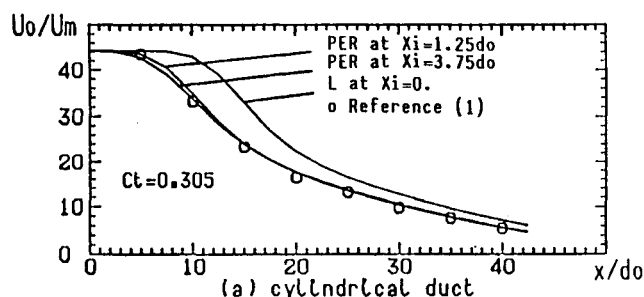


Fig. 3 Jet centerline velocity decay.

tic flow is carried out with the solution algorithm of Benodekar et al.<sup>7</sup>

Exploratory tests are conducted for several mesh sizes:  $22 \times 16$ ,  $32 \times 20$ ,  $42 \times 24$ , and  $52 \times 34$ . The results with the last two grid systems are essentially the same. Thus, the  $42 \times 24$  computation can be considered to be grid independent. Further details of the numerical methods employed are given in Ref. 8.

The results concerning  $U$ ,  $\overline{uv}$ ,  $r_1$ , and  $r_2$  obtained with the mixing length model in the parabolic computation are in close agreement with those obtained with the  $k-\epsilon$  model and with the available experimental results.<sup>8</sup> The simpler model is therefore adequate for this computation.

The performance of the PER scheme for the two confined jets is illustrated in Fig. 3. It is seen that good agreement with the experimental results is obtained if the parabolic computation is carried out over a distance  $x_i \approx 1d_0$ ; there is only a slight change if this computation is extended to  $3d_0$ . Particularly remarkable is the improvement of predictions for the diverging duct where the other upstream boundary conditions predicted a curve of a different shape. The time required for the parabolic computation is negligible compared to that of the elliptic flow (less than 1%).

## Conclusion

It is shown that the PER scheme, based on a parabolic computation of the upstream boundary condition for an elliptic flow, leads to notable improvements in the prediction of confined jets. The additional computational effort is minimal and no arbitrary adjustments are required. A simple mixing length model may be adequate for this purpose. The results presented here encourage the application of this scheme to other flows presenting similar difficulties.

## References

- <sup>1</sup>Barchilon, M. and Curter, R., "Some Details of the Structure of an Axisymmetric Confined Jet with Back-Flow," *Journal of Basic Engineering*, Vol. 86, No. 4, 1964, pp. 777-787.
- <sup>2</sup>Binder, G. and Kian, K., "Confined Jets in a Diverging Duct," *Proceeding of 4th Symposium on Turbulent Shear Flows*, Karlsruhe, FRG, Sept. 1983, pp. 7.18-7.23.
- <sup>3</sup>Schlichting, H., *Boundary Layer Theory*, McGraw-Hill, New York, 1969, Chap. 20.
- <sup>4</sup>Iacovides, H. and Launder, B. E., "PSL: An Economical Approach to the Numerical Analysis of Near Wall, Elliptic Flow," *Journal of Fluids Engineering*, Vol. 106, 1984, pp. 241-242.
- <sup>5</sup>Rajaratnam, N. and Pani, B. S., "Turbulent Compound Annular Shear Layers," *Journal of the Hydraulics Division, Proceedings of ASCE*, Vol. 98, No. HY7, July 1972, pp. 1101-1115.
- <sup>6</sup>Pletcher, R. H., "On a Finite-Difference Solution for the Constant-Property Turbulent Boundary Layer," *AIAA Journal*, Vol. 7, Feb. 1969, pp. 305-311.
- <sup>7</sup>Benodekar, R. W., Goddard, A. J. H., Gosman, A. D., and Issa, R. I., "Numerical Prediction of Turbulent Flow over Surface-Mounted Ribs," *AIAA Journal*, Vol. 23, March 1985, pp. 359-366.
- <sup>8</sup>Zhu, J., "Calcul des Jets Turbulents Confinés avec Recirculation," These de Doctorat de l'Institut National Polytechnique de Grenoble, France, 1986.

## Rayleigh Measurements of Species Concentration in a Complex Turbulent Flow

W. A. de Groot,\* R. Latham,\*  
J. I. Jagoda,† and W. C. Strahle‡  
Georgia Institute of Technology, Atlanta, Georgia

## Introduction

SOLID-FUELED ramjets (SFRJ) require a flame-anchoring region at the head of the combustion chamber, as do other ramjets. This low-velocity region in which air and pyrolyzed fuel are allowed to mix may be achieved by generating a recirculation zone behind a backward-facing step. The laboratory at Georgia Tech is currently investigating the complex flowfield over a backward-facing step with a bleed flow from the floor behind the step, for both cold flow and flow with combustion. A schematic of this SFRJ simulator is shown in Fig. 1. The bleed flow from the lower wall simulates the gases emanating from a solid fuel. As previously reported,<sup>1</sup> mean velocities, turbulence intensities, and shear stresses have been calculated using a modified  $k-\epsilon$  model and measured using a laser Doppler velocimeter (LDV) for the cold flow. Also calculated were the injectant mass fraction distributions in the cold

Received July 28, 1986; revision received Nov. 23, 1986. Copyright © American Institute of Aeronautics and Astronautics, Inc., 1987. All rights reserved.

\*Research Engineer, School of Aerospace Engineering.

†Associate Professor, School of Aerospace Engineering.

‡Regents' Professor, School of Aerospace Engineering.

flowfield. The manner in which the fuel loads up in the recirculation zone ultimately determines the temperature distribution in such a flowfield. It would, therefore, be useful to know the accuracy of the predicted mass fractions and mass transport rates. This Note is concerned with the measurement of the injectant concentration field using molecular Rayleigh scattering, and its comparison with prior analysis. This work is currently being extended to simultaneous measurements of the velocity and concentration in the cold flow and the velocity, concentration, and temperature determinations, using Raman scattering, in the flow with combustion.

### Experimental Work

The tunnel used in this investigation (Fig. 1) has previously been described in detail.<sup>1</sup> Briefly, air is drawn from the laboratory, passes over a backward-facing step, and establishes a recirculation zone. A secondary gas (air, CO<sub>2</sub>, or H<sub>2</sub>) can be bled into the recirculation zone through a porous floor. In the present study, a CO<sub>2</sub>/air mixture was used as the bleed gas because the scattering cross section of CO<sub>2</sub> is 2.4 times that of air. The tank from which the secondary flow was bled contained, at first, air at atmospheric pressure and was then filled to 100 psi using compressed CO<sub>2</sub>. In order to conserve the bleed gas, injection was limited to a region between two and eight step heights behind the step. Optical access was provided through anti-reflection coated glass sidewalls.

Concentrations of bleed gas were measured at various locations in the recirculation zone and the shear layer using Rayleigh scattering. The 488 nm beam from a 5 W argon ion laser was focused into the test section through the glass windows. Scattered light was collected using an F/10 lens and focused, through an interference filter, on a 500  $\mu$ m diameter pin hole placed in front of a photomultiplier (EMI 9813B). The output from the photomultiplier was passed through an amplifier (NEFF 122) and an A/D converter (Preston GMFD-2A) to an HP A700 computer. The 514.4 nm beam of the argon ion laser was used in an LDV system (TSI 9100-7) to eventually measure vertical velocities and concentrations simultaneously. The optical systems are mounted on a remotely controlled actuator. Concentration measurements can be carried out down to 0.1 step heights above the surface before reflections from the porous surface interfere with the concentration measurements. This system permits either pure concentration or simultaneous velocity and concentration measurements. The latter is of interest because it yields the correlation between the fluctuations in velocities and concentrations and, thus, the mass transport rates. The work on the simultaneous measurements is still in progress and, therefore, only pure Rayleigh results will be reported here.

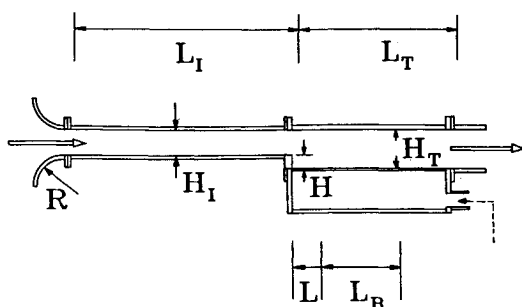


Fig. 1 Schematic of the backward-facing step facility where  $L_I$  (=61.6 cm) and  $H_I$  (=7.0 cm) are the length and height of the boundary-layer development section,  $L_T$  (=43.2 cm) and  $H_T$  (=10.5 cm) the length and height of the test section,  $H$  (=3.5 cm) the step height,  $R$  the bell mouth radius,  $L$  (=7.0 cm) the solid floor between the step and the injection plate, and  $L_B$  (=28.0 cm) the length of the injection plate; the tunnel is 41.9 cm wide. The main gas and bleed gas flow directions are shown as solid and dotted arrows, respectively.

Data from the Rayleigh detector were collected either continuously or triggered off the validated LDV outputs in preparation for the combined LDV/Rayleigh measurements. The Rayleigh data were transferred at a rate of 125,000 data points/s into the memory of the computer. At each location, 32,000 data points were collected and processed into pdf's from which the mean and rms of the concentrations were determined. In the latter case, 20 Rayleigh points at 8  $\mu$ s intervals were collected before and after each validated velocity measurement, averaged, and stored with their velocity values. Rejected were signals above a threshold voltage selected to discard any Mie scattering from particles in the test volume, while still accepting those from pure CO<sub>2</sub>. The low seed rate required for a successful determination of the

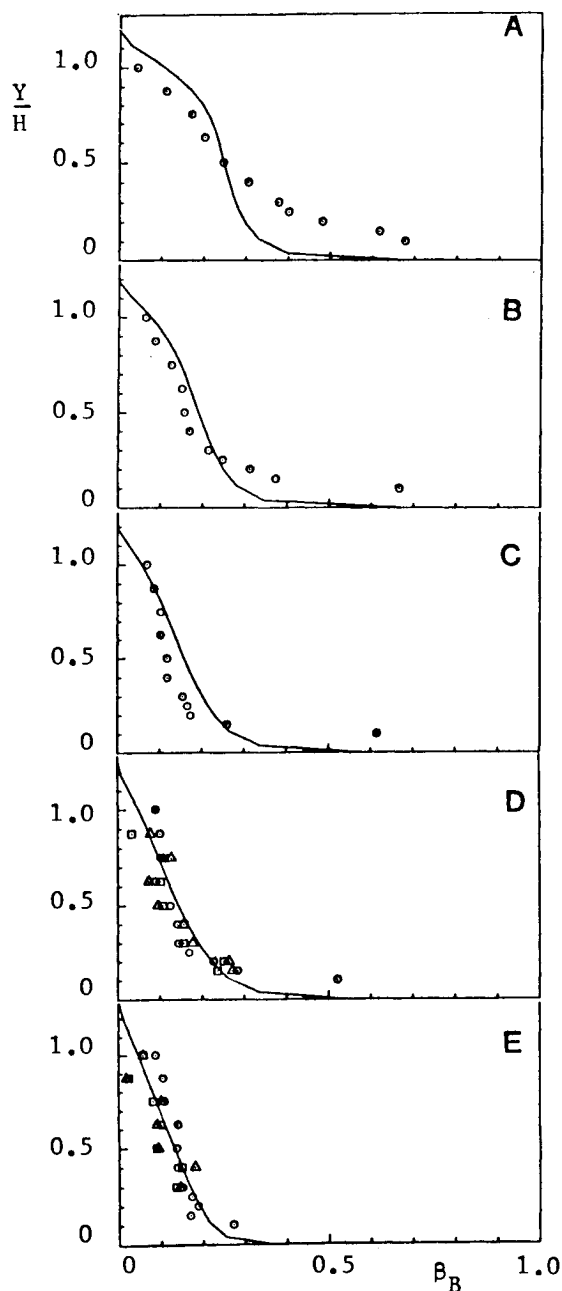


Fig. 2 Concentration of bleed gas vs height above the tunnel floor for CO<sub>2</sub>/air mixture as injectant at different axial locations: a) 2.9, b) 4.4, c) 5.9, d) 7.3, and e) 8.8 step heights ( $\circ$  and  $\square$  continuous data acquisition,  $\Delta$  seed particle triggered data acquisition, — predicted using  $k-\epsilon$ ).

CO<sub>2</sub> concentration resulted in a typical data rate of 10–50 points/s. Since a full tank of CO<sub>2</sub> provided only a 30 min run time, only 1000 LDV-triggered concentrations were measured for each position. Comparison of continuous and LDV-triggered concentration measurements permitted a check for a possible concentration bias toward higher air concentrations. Such a bias could have been possible when the Rayleigh signal was accepted only as a seed particle passed through the test volume since only the air could be seeded.

Previous Rayleigh measurements<sup>2,3</sup> had been carried out under ideal conditions. Because of the geometry of the tunnel, the LDV measurements had to be made in backscatter, while the optical axis of the Rayleigh detection system had to be placed at an angle of 27.5 deg to the incident laser beam and not at right angle for minimum Mie scattering noise from the dust particles in the flow. In addition, the  $F$  number of the Rayleigh collection lens was limited to 10 because of the short height and large width of the tunnel required to assure two-dimensional flow. In addition, the Rayleigh scattering measuring volume was often located in the immediate vicinity of the porous plate and surrounded by scattering surfaces that significantly increased the background scatter. This noticeably reduced the signal-to-noise ratio. Finally, and most significantly, the air drawn into the tunnel from the laboratory contained a large number of dust particles, which caused a widening and skewing of the pdf's.

These effects were taken into account in the data reduction procedures. For a mixture of pure bleed gas and air with no background scattering, the mole fraction of bleed gas  $\beta_B$  is given by

$$\beta_B = \frac{S_M - S_A}{(R - 1)S_A} \quad (1)$$

where  $S_M$  and  $S_A$  are the local scattered intensities due to the flow in the tunnel with and without bleed, respectively, and  $R$  the scattering ratio of pure bleed gas to air. The molar fraction of air  $n_A$  and of CO<sub>2</sub>  $n_C$  in the bleed gas are then calculated from the pressure in the supply tank using the perfect gas law.  $R$  is then given by

$$R = \frac{2 \cdot 4n_C + n_A}{n_C + n_A}$$

since the scattering ratio between pure CO<sub>2</sub> and pure air is 2.4.<sup>4</sup>

The measured scattering signal  $S'$  contains not only scattering from the gas  $S$ , but also background glare  $S_G$  and Mie scattering from particles  $S_D$ , such that  $S' = S + S_G + S_D$ . Equation (1) may then be rewritten as

$$\beta_B = \frac{S'_M - S'_A}{(R - 1)S'_A} \quad (2)$$

This assumes that at each location the contribution due to glare and dust is the same with and without bleed. The glare assumption appears to be clearly valid. Whether the particles contribute independently of the local bleed gas concentration can be determined by comparing the continuous Rayleigh results with those obtained when triggering off the particles. In the latter case, a bias toward lower bleed gas concentrations would be noted if the dust was predominantly concentrated in the air component.

The measurements were carried out first without the bleed gas  $S'_A$ , then with the bleed on  $S'_M$ , and then, once again, with the bleed off for comparison. In addition, a scattering value was obtained for relatively dust free air from a compressed air supply  $S_A$ . Since even this air was not entirely dust free, a correction had to be applied to  $S_A$  such that continuity is satisfied at the reattachment point using the previously obtained<sup>1</sup> axial velocity distribution at that station. Instantaneous values of  $S'_M$  and mean values of  $S'_A$  and  $S_A$  were substituted into Eq. (2) and a number of mass frac-

tions of bleed gas were obtained at each point and then processed into pdf's from which mean and rms bleed gas concentrations were calculated.

## Results and Discussion

Local bleed gas concentrations were measured for an axial inlet velocity of 70 m/s and a bleed gas velocity of 0.5 m/s, which corresponds to a typical gasification rate of the fuel in the SFRJ. None of the pdf's obtained were bimodal, indicating that the residence times in the recirculation zone were long enough for molecular mixing to prevent any pockets of pure bleed gas to be observed above 0.1 step height above the bleed plate.

Figure 2 shows the mean concentration of bleed gas vs height above the bleed plate at 2.9, 4.4, 5.9, 7.3, and 8.8 step heights downstream from the step. The first three stations lie within the recirculation zone with reattachment at 6.7 step heights for this flow. The circles and squares correspond to two separate runs using continuous Rayleigh measurements, while the triangles represent data collected by triggering off the seed particles via the LDV. The solid line was obtained from previously reported calculations using a modified  $k-\epsilon$  model.<sup>1</sup> Good agreement was observed between the measured and calculated bleed gas concentrations, except that the concentration gradient was somewhat underpredicted in the forward part of the recirculation zone and slightly overpredicted near the reattachment. This suggests that near the reattachment point the main and bleed gases are slightly better mixed than predicted, while close to the step the mixing process seems more diffusion controlled. This observation is in close agreement with the expectations from the velocity measurements.<sup>1</sup>

In addition, the data obtained in all three runs agree to within experimental accuracy. The excellent agreement between the data obtained from the continuous and velocity-triggered Rayleigh measurements is of particular importance for the simultaneous velocity/concentration measurements currently being carried out. Clearly, no significant bias in the mean concentration values is introduced by measuring the bleed gas levels only in the vicinity of seed particles. However, a close inspection of the shape of the concentration pdf's indicates a small change in the contribution to the pdf by the dust particles depending on the local concentration of the bleed gas. While this discrepancy does not appear to affect the mean concentrations, it has a significant effect on the calculation of the covariance of the velocity and concentration fluctuations. A more sophisticated data reduction technique in which the contributions of the electronic noise, the background glare, and the dust particles can be subtracted out is, therefore, currently under development for the combined measurements.

## Acknowledgments

Mr. Ronald E. Walterick was responsible for facility development and Mr. Fang-Hei Tsau provided the calculations presented in this paper. Mr. B. Misiak assisted with the experimentation. This work was sponsored by the Air Force Office of Scientific Research under Contract AFOSR-83-0356.

## References

- Richardson, J., de Groot, W. A., Jagoda, J. I., Walterick, R. E., Hubbart, J. E., and Strahle, W. C., "SFRJ Simulator Results: Experiment and Analysis in Cold Flow," *Journal of Propulsion and Power*, Vol. 1, Nov.-Dec. 1985, pp. 488-493.
- Driscoll, J. F., Schefer, R. W., and Dibble, R. W., "Mass Fluxes  $\rho'u'$  and  $\rho'v'$  Measured in a Turbulent Nonpremixed Flame," *Nineteenth Symposium (International) on Combustion*, The Combustion Institute, Pittsburgh, PA, 1982, pp. 477-485.
- Schefer, R. W. and Dibble, R. W., "Simultaneous Measurements of Velocity and Density in a Turbulent Nonpremixed Flame," *AIAA Journal*, Vol. 23, July 1985, pp. 1070-1078.
- Penny, C. M., "Light Scattering in Terms of Oscillator Strengths and Refractive Indices," *Journal of Optical Society of America*, Vol. 59, 1969, pp. 34-38.